IEEE Access
Multidisciplinary | Rapid Review | Open Access Journal

Received November 28, 2020, accepted December 16, 2020, date of publication December 25, 2020,
date of current version January 11, 2021.

Digital Object Identifier 10.1109/ACCESS.2020.3047408

Beam Split Algorithm for Height Measurement With Meter-Wave MIMO Radar

CHEN CHEN, JIANFENG TAO, GUIMEI ZHENG, AND YUWEI SONG
Air Defense and Missile Defense Academy, Air Force Engineering University, Xi'an 710051, China

Corresponding author: Guimei Zheng (zheng-gm@163.com)

This work was supported in part by the Young Talent Fund of University Association for Science and Technology in Shaanxi of China under Grant 20180109, in part by the Natural Science Basic Research Plan in Shaanxi Province of China under Grant 2019JM-155, and in part by the National Natural Science Foundation of China under Grant 61971438

ABSTRACT In order to improve the feasibility of low-elevation height measurement for meter-wave multiple-input multiple-output (MIMO) radar, a virtual sub-array-level beam splitting low-elevation height measurement algorithm is proposed. The algorithm can solve the coherence problems caused by low-angle multipath reflection, target reflection wave and direct wave coupling, and quickly measure the low elevation angle of the target on a flat ground, and then obtain the target height through the geometric relationship. First, establish an error graph in advance according to the radar frequency, antenna height and reflection coefficient; then combine the nine virtual channels of the three-element MIMO radar into three channels; then use the phase difference between adjacent channels to perform low-elevation encoding to confirm the target elevation range; The calculated amplitude error value is compared with the error curve diagram established in advance to obtain the target low elevation angle; finally, the target height data is obtained according to the geometric relationship. The signal model and error formula under complex terrain are finally derived. The simulation verifies the accuracy and superiority of the proposed algorithm on flat ground and complex undulating ground.

INDEX TERMS MIMO radar, beam split, low elevation angle, meter wave radar, angle estimation.

I. INTRODUCTION

The wavelength of the meter wave radar is generally in the meter wave band. Because of its long wavelength, it has natural advantages in anti-stealth, anti-radiation missiles, air defense early warning, etc. However, the meter wave radar has a wide beam and strong ground reflection. When detecting low-altitude targets, it will encounter coherent multipath signals, low Signal-to-noise ratio(SNR) and other issues [1]–[5]. So its low elevation angle measurement accuracy is lower, making it impossible to meet the needs of low altitude target detection. Therefore, the issue of meter wave radar height measurement has attracted the attention of many well-known scholars. Many researches on the height measurement of conventional phased array radar have been conducted. In [6], A method of height measurement based on beam splitting is proposed, which is simple, practical and conducive to engineering realization. Paper [7] derives a meter wave radar multipath signal model under complex terrain, and proposes a new height estimation method based on Alternate Projection(AP). This algorithm takes into account the influence of complex terrain and reduces the complexity of the algorithm. Paper [8] applies neural network technology in the field of conventional phased array meter wave radar, and obtained good angle measurement accuracy. Paper [9] proposes a low-elevation estimation method for wideband radar based on super-resolution algorithm, which is more suitable for complex terrain than the low-elevation estimation method of narrowband radar.

Compared with conventional phased array radars, Multiple-input Multiple-output (MIMO) radar, by adopting waveform diversity technology, gains advantages in angle measurement accuracy, anti-interference ability, anti-stealth effect, and multi-target tracking ability [10]–[13]. Therefore, the use of MIMO radar for low elevation angle estimation has become a development trend today, and hence has attracted the attention of many researchers [14]–[17]. Compared with the conventional meter-wave phased array radar, one target of the meter-wave MIMO radar corresponds to four transmission paths [18], [19], which causes the meter-wave

The associate editor coordinating the review of this manuscript and approving it for publication was Manuel Rosa-Zurera.

MIMO radarto have the problem of coherent sources as well as mutual penetration of steering vectors. Super-resolution algorithms are mainly divided into two categories. The first category is a subspace algorithm represented by Multiple Signal Classification (MUSIC) algorithms [20]. Because of the existence of multipath coherent signals, elevation angle estimation performance of this type of algorithm is poor. Although the spatial smoothing technique [21] can alleviate the coherence problem, it is at the expense of array aperture. In order to solve this problem, paper [22] proposes a generalized MUSIC algorithm. This paper constructs a steering matrix that is still orthogonal to the noise subspace when coherent sources exist, and obtains good angle measurement accuracy. In addition, paper [23] proposes to use polarization smoothing algorithm to process the echo signal, and then use the generalized MUSIC algorithm to solve the coherence problem of low-altitude targets. This method uses the geometric information of the symmetrical multipath model to reduce the amount of calculation and can solve the application problem of meter wave radar altitude measurement under extreme conditions. The second category is the maximum likelihood (ML) algorithm [24], [25], which can process coherent signals without decoherence processing, so it can be directly applied in MIMO radar and has good angle measurement accuracy. However, the computational complexity of this algorithm is too high. In order to reduce the computational complexity, the AP technique [26] is introduced to implement the ML estimation algorithm. In addition, paper [27], [28] uses prior information such as target distance, radar height, and surface reflection coefficient to reduce the number of unknown parameters, so that only one-dimensional search is performed on the target height. Prior information helps to improve performance and reduce the amount of calculation, but it is difficult to obtain in practical applications.

In recent years, many excellent height measurement algorithms have been proposed on the basis of the aforementioned low-angle target height measurement methods. Paper [19] proposes a ML method based on the beam space of the MIMO radar virtual array. Compared with the conventional ML estimation algorithm, this method has a lower calculation amount and better performance. In addition, paper [29] proposes a fast low-angle target estimation method for MIMO radar with arbitrary array configuration. This method has a small amount of calculation, but the accuracy of angle measurement is low under low SNR. In order to make full use of the energy of multipath signals, paper [14] and [30] proposes a peak search algorithm of low-angle estimation based on multipath echo signal power and MIMO radar spatial diversity. This algorithm makes full use of the energy of multipath signals and can measure the elevation angle of low-altitude targets without decoherence. Time reversal (TR) technology can make full use of the energy of multipath signals, so paper [31] proposes an adaptive time reversal beam space MUSIC (ATR-BSMUSIC) algorithm, which does not require decoherence processing and has a low computational load. In order to solve the influence of color noise, paper [18] uses the covariance difference method to eliminate the color noise, then uses the matrix reconstruction method to eliminate the interference of the multipath signal, and finally uses the unitary Estimation of Signal Parameter via Rotational Invariance Technique (ESPRIT) algorithm to obtain the elevation angle. Paper [15] considers both transmission and reception multipaths, and proposes a height estimation method based on rank 1 constraint and sparse representation. In both simple multipath and complex multipath situations, this method can effectively improve the accuracy of target height estimation.

The algorithms proposed in the above documents all have good angle measurement accuracy, but their application in engineering is limited due to the large calculation load. In order to further reduce the practical application difficulty of low elevation angle estimation for meter-wave MIMO radar, this paper proposes a virtual sub-array-level beam splitting height measurement algorithm for MIMO radar based on the paper [6]. Simple and practical, this method can quickly obtain the target low elevation angle, and can be easily implemented in engineering. The specific procedures of this method are as follows. Firstly, MIMO radar is proved to have the phenomenon of beam splitting in the low-elevation area; then the target elevation range is determined by the phase difference of adjacent elements; then according to the error graph, the actual error signal value is extracted by the error formula to obtain the low elevation angle of the target; finally the geometric relationship is analyzed to obtain the height of the target.

The rest of this paper is organized as follows. Section II derives a signal model suitable for MIMO radar beam splitting algorithm. Section III derives and analyzes the MIMO radar virtual subarray beam splitting algorithm proposed in this paper in detail, and lists the algorithm steps. Section IV derives the signal model and the corresponding error value formula of the proposed algorithm under complex terrain, and uses many simulation experiments to verify it. In Section V, the performance of the proposed method is verified through a large number of simulations. Section VI summarizes the conclusions of this paper.

II. SIGNAL MODE

Assume a monostatic MIMO radar system with M sensors installed vertically on the horizontal plane. The transmitted signal is a set of orthogonal signals $\varphi(t) \in C^{M\times 1}$, and the height of the array element is $H_k, k = 1, \ldots, M$. Assuming that the height and elevation of the target are H_T and β, the slant distance between the target and the antenna is R, and the incident angle of the direct wave is θ_d, and the reflection angle is θ_i, respectively. If condition $R \gg H_T$ is met, equation $\beta \approx \theta_d \approx -\theta_i$ exists [22]. When the signal reaches the target, $R_{rd,k}$ and $R_{ri,k}$ are the lengths of the direct path and the indirect path from the signal to the kth antenna [6], respectively. The direct path and reflected path from the target to the kth antenna are $R_{rd,k}$ and $R_{ri,k}$. Respectively,if the receiving antenna and the transmitting antenna are shared,

the relationship $R_{td,k} = R_{rd,k}$ and $R_{ti,k} = R_{ri,k}$ are established. According to the geometric relationship, the direct path and the reflected path can be expressed as follows:

$$\begin{aligned} R_{td,k} &= R_{rd,k} = \sqrt{R^2 - H_T^2 + (H_T - H_k)^2} \\ &= \sqrt{R^2 - 2RH_k \sin\beta + H_k^2} \\ &\approx \sqrt{R^2 - 2RH_k \sin\beta + (H_k \sin\beta)^2} \\ &= R - H_k \sin\beta \end{aligned} \tag{1}$$

$$R_{ti,k} = R_{ri,k} = \sqrt{R^2 - H_T^2 + (H_T + H_k)^2} \approx R + H_k \sin\beta \tag{2}$$

From formula (1) and (2), the expression of the signal arriving at the target can be derived as follows

$$\begin{aligned} & x(t,\beta) \\ &= \sum_{k=1}^{M} \left[\exp\left(-j\kappa R_{td,k}\right) + \Gamma \exp\left(-j\kappa R_{ti,k}\right)\right]\varphi_k(t) \\ &\approx \sum_{k=1}^{M} \left[j2\sin(\kappa H_k \sin\beta)\exp\left(j\left(-\kappa H_k \sin\beta - \kappa R\right)\right)\right]\varphi_k(t) \\ &= \sum_{k=1}^{M} \left[2\sin(\kappa H_k \sin\beta)\exp\left(j\left(\frac{\pi}{2} - \kappa H_k \sin\beta - \kappa R\right)\right)\right] \\ &\quad \times \varphi_k(t) \\ &= A_t^T Z(t) \end{aligned} \tag{3}$$

In formula (3), $\kappa = 2\pi/\lambda$, Γ is the horizontal polarization reflection coefficient, which is taken as -1. In addition, in order to simplify the formula, there are the following settings: $A_t = \begin{bmatrix} 2\sin(\kappa H_1 \sin\beta)\exp(-j\kappa H_1 \sin\beta), \ldots, \\ 2\sin(\kappa H_k \sin\beta)\exp(-j\kappa H_k \sin\beta) \end{bmatrix}^T$, $k = 1, \ldots, M$, $Z(t) = \exp\left(j\left(\frac{\pi}{2} - \kappa R\right)\right)\varphi(t)$. After further deduction, the data received by the m-th receiving array element can be expressed as

$$\begin{aligned} & s_m(t,\beta) \\ &= \left[\exp\left(-j\kappa R_{rd,m}\right) + \Gamma \exp\left(-j\kappa R_{ri,m}\right)\right]x(t,\beta) \\ &\quad + n_m(t) \approx j2\sin(\kappa H_m \sin\beta)\exp\left(j\left(-\kappa H_m \sin\beta - j\kappa R\right)\right) \\ & x(t,\beta) + n_m(t) \\ &= 2\sin(\kappa H_m \sin\beta)\exp\left(j\left(\frac{\pi}{2} - \kappa H_m \sin\beta - \kappa R\right)\right) \\ & x(t,\beta) + n_m(t) \\ &= A_{r,m} A_t Z(t) + n_m(t) \end{aligned} \tag{4}$$

where $n_m(t)$ is Gaussian white noise. Since it is assumed that the receiving antenna and the transmitting antenna are shared, the received data of the entire receiving array can be approximately expressed as

$$S(t,\beta) = A_r A_t^T Z(t) + n(t), \quad \in C^{M\times 1} \tag{5}$$

Using the orthogonality between the transmitted signals, the output of the above received data processed by a set of matched filters can be expressed as:

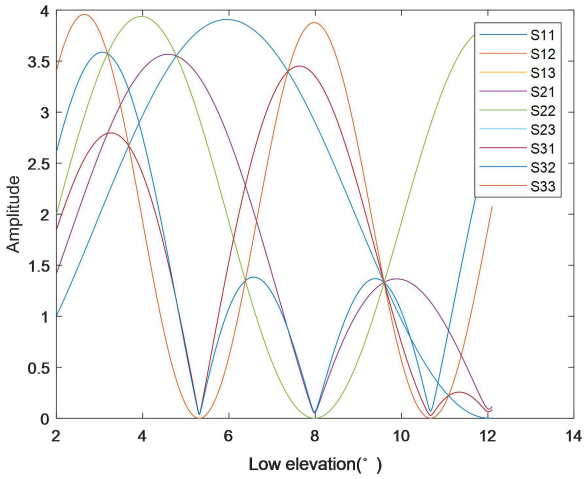

FIGURE 1. MIMO radar beam splitting diagram.

$$\begin{aligned} S &= \int S(t,\beta)\varphi(t)^H \\ &= A_r A_t^T \exp\left(j\left(\pi - 2\kappa R\right)\right) + N(t), \quad \in C^{M\times M} \end{aligned} \tag{6}$$

The element in the mth row and kth column in formula (6) is the reflection data of the kth transmitting array element received by the mth receiving array element through the target and the ground:

$$\begin{aligned} \mathrm{S_{m,k}} &= 4\sin(\kappa H_m \sin\beta)\sin(\kappa H_k \sin\beta) \\ &\quad \times \exp\left(j\left(\pi - 2\kappa R - \kappa(H_k + H_m)\sin\beta\right)\right) \end{aligned} \tag{7}$$

When the radar operating frequency is 180MHz and the antenna height is $H_1 = 4m$, $H_2 = 6m$, $H_3 = 9m$ respectively, the beam splitting diagram shown in Fig. 1 can be obtained.

It is not difficult to find from Fig. 1 that it has a beam splitting phenomenon, but its beam is lossy and messy. Observation shows that when m = k, it has a strict beam splitting phenomenon, and there is no loss phenomenon, is shown in the following formula.

$$S_{k,k} = 4\sin(\kappa H_k \sin\beta)^2 \exp\left(j\varphi_{k,k}\right) \tag{8}$$

$$\left|S_{k,k}\right| = 4\sin(\kappa H_k \sin\beta)^2 \tag{9}$$

where $\varphi_{k,k} = \pi - 2\kappa R - 2\kappa H_k \sin\beta$, observing formulas (8) and (9), we can find:

(1) When formula $\kappa H_k \sin\beta = n\pi$ is established (n is an integer), formula $\left|S_{k,k}\right| = 0$ is established. At this time, the received data amplitude is 0, which leads to a blind zone in the angle measurement; when $\sin\beta = (2n+1)\lambda/(4H_k)$ and $\sin\beta = n\lambda/(2H_k)$ are established, the amplitude of the received data signal is at the peak and trough positions. It is not difficult to find that the positions of the peaks and troughs are related to the wavelength and the height of the antenna.

(2) The phase angle of $\kappa H_k \sin\beta$ is in the interval between $(2n\pi, (2n+1)\pi)$ and $((2n+1)\pi, (2n+2)\pi)$, that is, when $\sin\beta$ is in the interval $(n\lambda/H_i, (2n+1)\lambda/(2H_i))$ and $((2n+1)\lambda/(2H_i), (n+1)\lambda/H_i)$, the phase of $S_{k,k}$ is

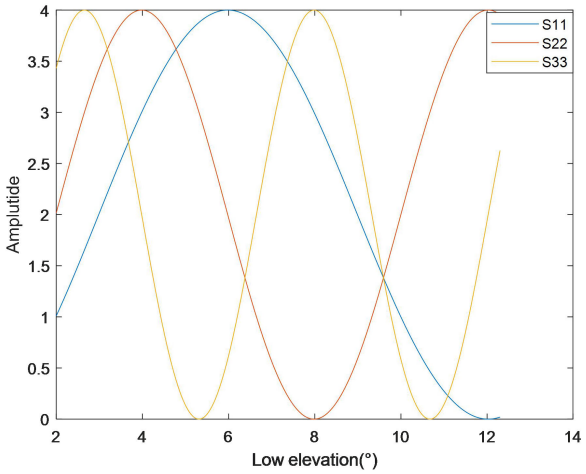

FIGURE 2. Beam splitting diagram of main element.

$\varphi_{k,k}$ or $\pi+\varphi_{k,k}$. respectively, it can be found that the adjacent beam splitting has a "phase inversion" relationship.

From the above analysis, it can be found that MIMO radar can also use beam splitting for low elevation angle measurement, and MIMO radar has the advantages of virtual aperture expansion, strong anti-interference ability, and high resolution. Therefore, the use of MIMO radar beam splitting for low elevation angles will increase measurement accuracy.

III. HEIGHT MEASUREMENT METHOD FOR METER WAVE MIMO RADAR BASED ON BEAM SPLITTING

A. BEAM SPLITTING ALGORITHM BASED ON MIMO RADAR MAIN ELEMENT

Consider a vertically-placed MIMO radar system, where the transceiver elements are shared and the number of elements is M = N = 3. According to the expansion characteristics of MIMO radar virtual array elements, it can expand the number of array elements from 3 to 9, and the data received by each virtual array element is as shown in equation (7). From the analysis in the previous section, it can be seen that MIMO radar also has beam splitting in the low-elevation area, but the received data of the 6 virtual array elements has attenuation, and the effect of directly applying the beam splitting method of conventional array radar is poor. Through observation, it can be found that the received data of the three main elements will not be attenuated. Therefore, this paper uses the three main elements to perform beam splitting angle measurement, that is, use the received data when m = k to perform angle measurement. Fig. 2 shows the beam splitting diagram of the three virtual array elements $S_{k,k}, k = 1, 2, 3$. It can be found from Fig. 2 that the crests and troughs of each antenna are staggered, and they are just complementary to cover the blind area of the angle measurement.

Assuming that the antenna height difference is much smaller than the radar range resolution. In the far-field condition, the signal emitted by the k-th transmitting antenna is received by the k-th receiving antenna after reflection, and the signal model is formula (8).

TABLE 1. Elevation angle coding diagram.

C_{12} C_{13} C_{23}	Elevation range
1 1 1	$2^\circ \sim 5.32^\circ$
1 0 0	$5.32^\circ \sim 8^\circ$
0 0 1	$8^\circ \sim 10.68^\circ$
0 1 0	$10.68^\circ \sim 12^\circ$

When formula $0 < \kappa H_k \sin\beta < \pi$ is established, here has formula $0 < \sin\beta < \lambda/(2H_k)$. At this time, the phase difference of the signals received by two adjacent array elements is:

$$\begin{aligned}\phi_{k,k+1} &= \Phi[S_{k+1,k+1}] - \Phi[S_{k,k}] \\ &\approx 2\kappa(H_{k+1} - H_k)\sin\beta \end{aligned} \tag{10}$$

In formula (10), Φ represents the phase angle obtained. It is not difficult to find that the target elevation angle can be obtained from formula (10), but it can be found from the periodicity of the sine function that the elevation angle obtained by directly using formula (10) will have multiple values. For example, $\lambda = 1.66\text{m}$ $H_k = 9\text{m}$ and $\beta > 5.3^\circ$, there will be multiple values at that time. Therefore, the range of elevation angle obtained only by the phase comparison method is too small, which is not suitable for practical applications.

In order to solve the above-mentioned multi-value problem and expand the angle measurement range, the elevation angle range of the target can be determined according to the phase difference encoding. It is found through experiments that the phase difference of S_{11}, S_{21}, S_{31} in the received data can be used to determine the elevation range of the target. Since the beam has a "phase inversion" phenomenon, the phase of S_{11}, S_{21}, S_{31} is $\varphi_{11}, \varphi_{21}, \varphi_{31}$ or $\pi+\varphi_{11}, \pi+\varphi_{21}, \pi+\varphi_{31}$. Its phase difference is

$$\begin{aligned}\phi_{1,2} &= \pm\pi + \kappa(H_2 - H_1)\sin\beta, \\ \phi_{1,3} &= \pm\pi + \kappa(H_3 - H_1)\sin\beta, \\ \phi_{2,3} &= \pm\pi + \kappa(H_3 - H_2)\sin\beta \end{aligned} \tag{11}$$

Take the sign function of the above formula to get

$$\begin{aligned} C_{i,j} &= sign\left[\cos\left(\phi_{i,j}\right)\right] = \begin{cases} 1, \cos\left(\phi_{i,j}^{`}\right) \geq 0 \\ 0, \cos\left(\phi_{i,j}^{`}\right) < 0, \end{cases} \\ & i = 1, 2; \quad j = 2, 3; \ i < j \end{aligned} \tag{12}$$

Use $C_{1,2}, C_{1,3}, C_{2,3}$ as the code to determine the elevation range. When the radar frequency is 180MHz and the antenna height is $H_1 = 4m$, $H_2 = 6m$, $H_3 = 9m$, the elevation angle code and the corresponding elevation angle range can be calculated in Table 1, When the elevation angle is greater than 12, there will be a multi-value phenomenon, but this angle range has satisfied the practical need of low elevation angle height measurement.

After we determine the target elevation angle interval, the following formula can be obtained by processing the amplitude ratio of the data received by different

array elements [32], which is called the error formula in this paper.

$$E_{i,j}(\beta) = \frac{|S_{i,1}| - |S_{j,1}|}{|S_{i,1}| + |S_{j,1}|}, \quad i = 1, 2\, j = 2, 3.i < j \tag{13}$$

Substituting formula (7) for the formula (13) to simplify and obtain

$$E_{i,j}(\beta) = \frac{\sin\left(\kappa\left(H_i + H_j\right)\sin\beta\right)\sin\left(\kappa\left(H_i - H_j\right)\sin\beta\right)}{1 - \cos\left(\kappa\left(H_i + H_j\right)\sin\beta\right)\cos\left(\kappa\left(H_i - H_j\right)\sin\beta\right)} \tag{14}$$

Observing the above formula, we can find that the error formula is related to the wavelength and antenna height. When measuring the elevation angle, you can first determine the radar operating frequency and the antenna height of each element. The following figure shows the error curve of the above formula. It can be seen that due to the existence of beams splitting, the following figure has a multi-value phenomenon, but it is a single value in each elevation angle coding interval, so we can first confirm the elevation angle range according to the elevation angle coding, and determine which one or two error curves to obtain the target elevation angle. In addition, because there is a jump phenomenon at the inflection point of the error curve, when selecting the error curve, the error curve with a large slope can be selected for search and comparison to improve the accuracy of angle measurement.

B. VIRTUAL SUBARRAY BEAM SPLITTING ALGORITHM BASED ON MIMO RADAR

The method proposed in the previous section can correctly measure the low elevation angle of the target. This method fails to reflect the advantages of the MIMO radar virtual extended array element, because it only uses the received data of the main virtual array element rather than other virtual array elements. Compared with the conventional array beam splitting algorithm, its angle measurement accuracy is not much improved,so it is not practically valuable. Therefore, this section proposes a virtual subarray beam splitting algorithm based on MIMO radar, making full use of the advantages of virtual extended array elements of MIMO radar.

Assuming a MIMO radar system with co-located transceivers, the number of receiving array elements is M = N = 3, and the number of virtual array elements can be expanded to 9. Each virtual array element receives data as in formula (7). The data received by the receiving element is equivalent to a sub-array with the number of elements M, so that N = 3 sub-arrays can be obtained. The three virtual array elements in the sub-array are combined into one channel to narrow the composite beam of the sub-array and improve the accuracy of angle measurement.

The vectorized operation of formula (6) can be obtained

$$S^{`} = vec(S) = A_r \otimes A_t^T \exp\left(j\left(\pi - 2\kappa R\right)\right) + vec(N(t)), \in C^{M^2 \times 1} \tag{15}$$

Define G as the sub-array synthesis matrix, whose value is

$$G = \begin{bmatrix} 1 & 1 & 1 & 0 & 0 & 0 & 0 & 0 & 0 \\ 0 & 0 & 0 & 1 & 1 & 1 & 0 & 0 & 0 \\ 0 & 0 & 0 & 0 & 0 & 0 & 1 & 1 & 1 \end{bmatrix} \tag{16}$$

Then the sub-array synthesis matrix can be used to combine the nine array element channels into three array element channels, and the signal vector is as follows

$$U(\beta) = GS^{`} = \begin{bmatrix} S_1^{`} + S_2^{`} + S_3^{`} \\ S_4^{`} + S_5^{`} + S_6^{`} \\ S_7^{`} + S_8^{`} + S_9^{`} \end{bmatrix} \in C^{M \times 1} \tag{17}$$

Same as section B, first obtain the elevation angle code according to the phase relationship of the three synthetic channels to determine the target elevation angle range, and then compare the synthetic channel error curves to obtain the target elevation angle.

The phase difference between adjacent channels is as follows

$$\phi_{i,j} = \Phi(U_i) - \Phi\left(U_j\right), \quad i < j, \begin{matrix} i = 1, 2 \\ j = 2, 3 \end{matrix} \tag{18}$$

Due to the existence of multipath effects, formula (16) has a phenomenon of beam splitting, that is, there is a phase inversion phenomenon, so formula (17) can be processed as follows

$$C_{i,j} = sign\left[\cos\left(\phi_{i,j}\right)\right] = \begin{cases} 1, \cos\left(\phi_{i,j}^{`}\right) \geq 0 \\ 0, \cos\left(\phi_{i,j}^{`}\right) < 0 \end{cases} \quad i < j, \begin{matrix} i = 1, 2 \\ j = 2, 3 \end{matrix} \tag{19}$$

Use $C_{1,2}, C_{1,3}, C_{2,3}$ as the code to determine the elevation angle range. When the frequency is 180MHz and the antenna height is $H_1 = 4m, H_2 = 6m, H_3 = 9m$, the elevation angle code calculated by the above formula and the corresponding elevation angle range are the same as Table 1.

After determining the range of elevation angle, use the comparing amplitude method to calculate the error value of the synthesized channel.

$$E_{i,j}(\beta) = \frac{|U_i| - |U_j|}{|U_i| + |U_j|}, \quad i < j, \begin{matrix} i = 1, 2 \\ j = 2, 3 \end{matrix} \tag{20}$$

Before low elevation angle estimation, the error curve is calculated according to formula (20) within the range of ($2^\circ \sim 12^\circ$) based on prior knowledge of radar wavelength, antenna height, ground reflection coefficient. Using formula (20), the error value $E_{1,2}(\beta)$, $E_{1,3}(\beta)$, $E_{2,3}(\beta)$ can be calculated. After confirming the target elevation angle range by using the elevation angle code, the low elevation angle of the target can be obtained by comparison to achieve the purpose of altitude measurement.

Suppose a vertical MIMO radar with co-located transceivers, the number of array elements is M = N = 3. When the antenna height becomes lower, the elevation measurement range of the algorithm becomes larger, but the angle measurement accuracy will decrease accordingly. The shorter

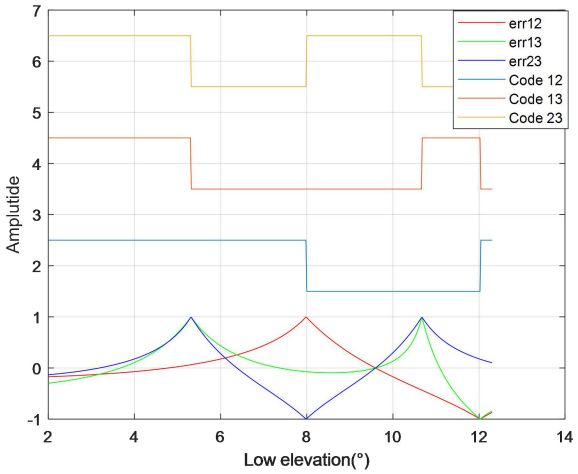

FIGURE 3. MIMO sub-array error curve.

the wavelength, that is, the lower the operating frequency of the radar will improve the accuracy of the angle measurement, but the angle measurement range will be reduced. In order to balance the accuracy and the angle measurement range, the antenna height is $H_1 = 4m$, $H_2 = 6m$, $H_3 = 9m$, the radar operating frequency is 180MHz, and the ground reflection coefficient is $\Gamma = -0.95$. From formula (19), the error graph of the virtual sub-array can be obtained as shown in Fig. 3. It can be found that the error graph of the virtual sub-array is sharper than the error graph of the main element and has a greater slope at the inflection point. Therefore, theoretically analyzed, the measurement angle accuracy will be higher.

The algorithm steps are as follows:

Step 1: Use the comparing amplitude method to establish an error graph,according to the working frequency of the MIMO radar, antenna height, and the terrain surrounding the radar;

Step 2: Use the sub-array synthesis matrix to synthesize the nine received signals into three received signals, and then calculate the elevation angle code according to equation (19) to determine the elevation angle range;

Step 3: Use equation (20) to calculate the error value of the actual received signal;

Step 4: Compare the actual error value with the error curve to measure the target elevation angle;

Step 5: Calculate the target height as

$$H \approx R \sin \beta + H_a \tag{21}$$

Among them, H_a is the antenna erection height;R is the elevation angle and β is the target distance.

IV. THE INFLUENCE OF TERRAIN ON SURVEY ACCURACY

It is not difficult to find that the accuracy of the beam splitting height measurement algorithm is mainly related to the SNR and the terrain conditions of the reflection point. This section mainly analyzes the influence of the terrain conditions of the reflection point on the measurement accuracy. In order to better analyze the performance of the proposed algorithm,

TABLE 2. Several typical media values.

medium	$\sigma/\Omega_\circ\ m^{-1}$	ε'	ε''
Dry ground	10^{-4}	4	0.006
Wet ground	10^{-2}	30	0.6
seawater	4.3	80	774
freshwater	10^{-3}~10^{-2}	78	0.06~0.6

define the root mean square error formula(RMSE) as follows:

$$RMSE = \frac{1}{P}\sqrt{\frac{1}{K}\sum_{k=1}^{K}\sum_{p=1}^{P}\left[\left(\hat{\theta}_{p,k} - \theta_p\right)^2\right]} \tag{22}$$

where: K is the number of Monte Carlo, P is the number of elevation angles within the range of elevation angle; $\hat{\theta}_{p,k}$ is the estimated value of the p-th elevation angle in the k-th experiment, and θ_p is the p-th elevation angle in the range of elevation angles. In this section, the Monte Carlo number K = 1000, and the target slope distance R = 200 km.

A. FLAT GROUND REFLECTION COEFFICIENT

The reflection coefficient of a flat ground can be determined by the Fresnel equation [33], [34], which is mainly determined by the electromagnetic wave frequency, polarization coefficient, grazing angle and surface type:

$$\rho_0 = \frac{\varepsilon_c^b \sin\psi - \sqrt{\varepsilon_c - (\cos\psi)^2}}{\varepsilon_c^b \sin\psi + \sqrt{\varepsilon_c - (\cos\psi)^2}} \tag{23}$$

In the formula, ε_c is the complex permittivity and ψ is the wiping angle. When b is 0, equation (23) is the horizontal polarization reflection coefficient, and when it is 1, it is the vertical polarization reflection coefficient. The value of the complex permittivity is related to the type of reflective ground:

$$\varepsilon_c = \frac{k}{\varepsilon_0} - j\frac{\sigma}{\omega\varepsilon_0} = \varepsilon' - j\varepsilon'' \tag{24}$$

In formula (24), ε_0 is the free space permittivity, k is the permittivity, σ is the conductivity, and the typical values of ε' and ε'' can be found in the relevant paper [35]. Several typical values are as follows

Since horizontally polarized waves can increase the energy at the peak of the beam, this paper uses horizontally polarized waves. Under four different media, the RMSE of the angle of the virtual subarray algorithm proposed in this paper is shown in Fig. 4. It can be seen from Fig. 4 that under the condition of 10dB SNR, the algorithms proposed in this paper have good angle measurement accuracy under different media. The slightly larger error than other angles appears near 5.3° and 8° because it is near the inflection point of the error curve. Fig. 4 shows that before establishing the error curve, the correct reflection coefficient of the medium can improve the accuracy of angle measurement.

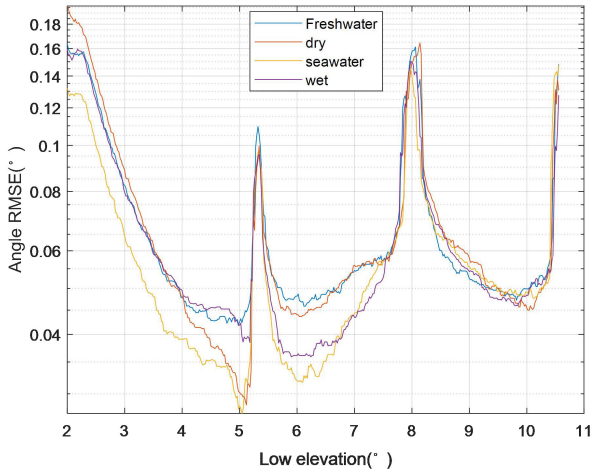

FIGURE 4. Angle RMSE of the proposed algorithm in different media.

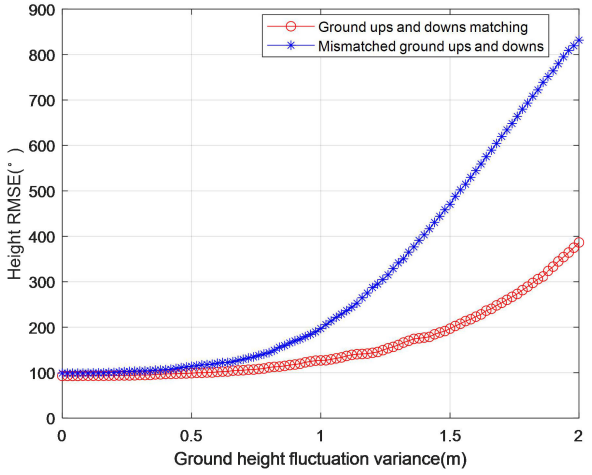

FIGURE 5. The height RMSE diagram with the degree of fluctuation.

B. ROUGH GROUND REFLECTION COEFFICIENT

In practice, the ground is uneven, that is, the ground has undulating characteristics. This makes the actual ground reflection coefficient mismatch with the flat ground reflection coefficient. When the following Rayleigh conditions are met, it can be considered as a relatively flat ground.

$$\sigma_{\mathrm{h}} \sin \psi < \lambda/8 \tag{25}$$

Rough surface reflection coefficient is determined by flat ground reflection coefficient ρ_0, diffusion factor D and coefficient γ [36]:

$$\rho = \rho_0 D \gamma \tag{26}$$

here, $\gamma = \exp\left[-2\left(\frac{2\pi}{\lambda}\sigma_h \sin\psi\right)^2\right]$, $D \approx \left(1+\frac{2G_1(G-G_1)}{r_e G \sin\psi}\right)^{1/2}$, here G is the horizontal distance between the target and the radar (on the surface of the earth); G_1 is the horizontal distance between the reflection point and the radar; r_e is the equivalent earth radius; σ_h is the standard deviation of the height fluctuation of the ground subject to the Gaussian distribution, indicating the roughness of the ground or the degree of fluctuation; D usually takes 1. In the case of rough ground and meeting the Rayleigh criterion, the received data after matched filtering can be expressed as

$$\begin{aligned} S_{m,k} = & \left[\exp\left(-j\kappa R_{rd,m}\right) + \rho \exp\left(-j\kappa R_{ri,m}\right)\right] \\ & * \left[\exp\left(-j\kappa R_{td,k}\right) + \rho \exp\left(-j\kappa R_{ti,k}\right)\right] + n_{m,k}(t) \end{aligned} \tag{27}$$

The formula of the amplitude error curve based on the MIMO main element can be expressed as

$$E_{i,j} = \frac{2\rho \sin\left(\kappa\left(H_i + H_k\right)\sin\beta\right)\sin\left(\kappa\left(H_i - H_k\right)\sin\beta\right)}{1+\rho^2-2\rho\sin\left(\kappa\left(H_i+H_k\right)\sin\beta\right)\cos\left(\kappa\left(H_i-H_k\right)\sin\beta\right)} \tag{28}$$

Fig. 5 is the height RMSE diagram of the algorithm proposed in this paper, which changes with the standard deviation of the ground ups and downs. The target low elevation angle is 4. The slope distance is 200km, and the SNR is 16dB. It can be found from Fig. 5 that when the degree of fluctuation increases, the height measurement error also increases. In addition, the error after terrain matching is greatly reduced. Therefore, it is necessary to match the surrounding terrain when establishing the error curve to obtain a good measurement accuracy. It is also found from the figure that the algorithm proposed in this paper is more suitable for terrain with small undulations.

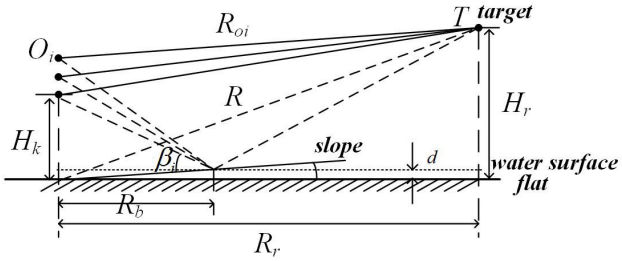

FIGURE 6. The geometric relationship of the tilt matrix.

C. THE INFLUENCE OF TILT ANGLE ON MEASUREMENT ACCURACY

In actual situations, it is difficult to have a completely flat ground. Therefore, this section will analyze the algorithm proposed in this paper with the existence of the tilt considered.

Assume that the angle of inclination between the ground reflection point and the horizontal plane is θ, which is positive when it is convex and negative when it is concave. For an antenna with a height of H_k, suppose the height of the ground reflection point is d, the horizontal distance from the antenna is R_b, the horizontal distance between the target and the radar is R_r, and the grazing angle is ψ, as shown in the fig. 6.

The following geometric relations can be derived:

$$\tan\psi = \frac{H_k - d}{R_b} = \frac{H_T + H_{\mathrm{k}}}{R_r} \approx \tan\beta \tag{29}$$

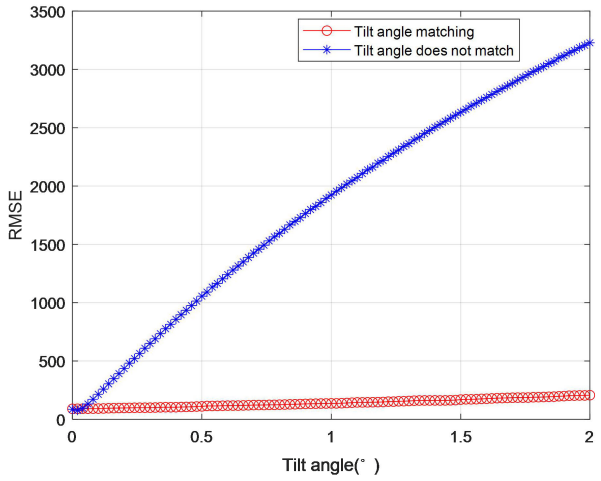

FIGURE 7. The height RMSE graph with tilt angle.

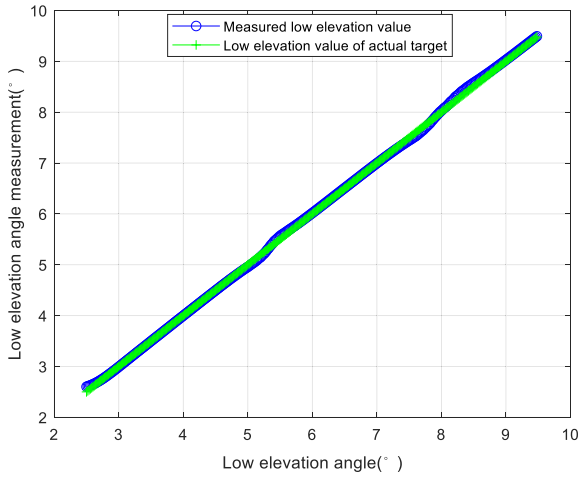

FIGURE 8. Comparison of measured angle and actual angle.

$$R_b \approx \frac{H_k - d}{\tan\beta} \tag{30}$$

$$d = R_b \tan\theta \approx \frac{H_i \tan\theta}{\tan\beta + \tan\theta} \tag{31}$$

At this time, the reflection path value from the antenna to the target and the reflection path value from the target to the antenna are

$$\begin{aligned} R_{ti,k} &= R_{ri,k} = \sqrt{R^2 - H_T^2 + (H_T + H_k - 2d)^2} \\ &\approx R + (H_k - 2d)\sin\beta \end{aligned} \tag{32}$$

At this time, considering the ground ups and downs, the ground reflection coefficient is ρ, and the error formula of the beam splitting based on the main array element is

$$E_{i,j} = \frac{2\rho \sin(\zeta_A)\sin(\zeta_B)}{1 + \rho^2 - 2\rho\cos(\zeta_A)\cos(\zeta_B)} \tag{33}$$

here has:

$$\xi_A = \kappa\left(H_{\mathrm{i}} + H_j\right) K_\theta \sin\beta \tag{34}$$

$$\xi_B = \kappa\left(H_{\mathrm{i}} - H_j\right) K_\theta \sin\beta \tag{35}$$

$$K_\theta = \frac{1}{1 + K_\theta^{\cdot}} = \frac{1}{1 + \tan\theta/\tan\beta} \tag{36}$$

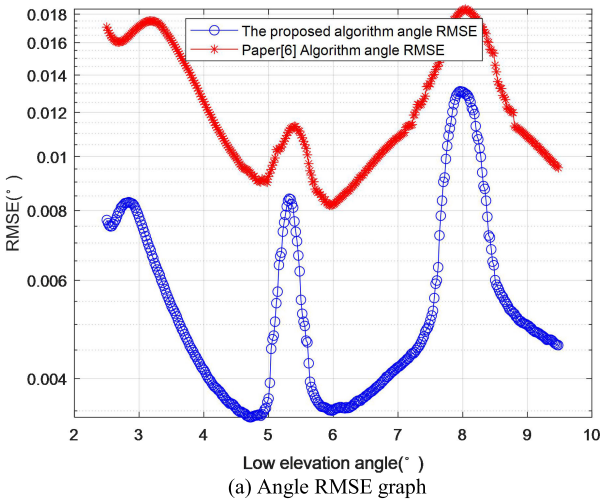

(a) Angle RMSE graph

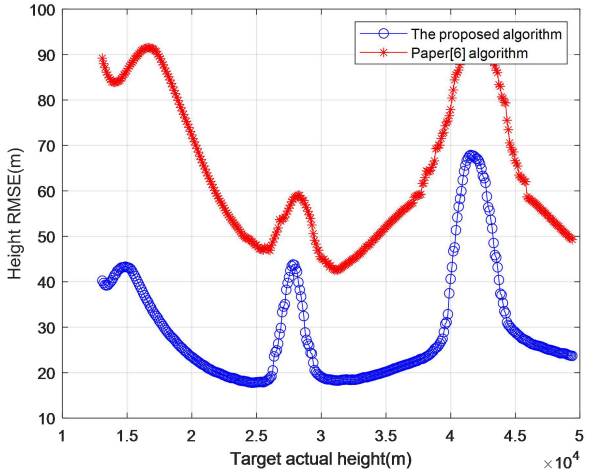

(b) Height RMSE graph

FIGURE 9. RMSE graph.

Here, let K_θ be the correction coefficient of the slope position;when $\theta < 5°$ holds, there is $K_\theta^{\cdot} = \tan\theta/\tan\beta \approx \theta/\tan\beta$, which represents the slope relative to the cotangent of the elevation angle.

When the ground undulation variance is 0.7 m, the height RMSE of the method proposed in this paper is shown in Fig. 7, which varies with the ground inclination angle. It can be seen from Fig. 7 that the height RMSE increases with the increase of the tilt angle, and the RMSE of the height after terrain matching is greatly reduced. Therefore, when performing altitude measurement, it is necessary to detect the terrain in advance and establish an error graph that matches the actual tilt angle to obtain an accurate target height. Although the RMSE is relatively small when establishing the matching error curve, the proposed method is more suitable for flat ground.

V. COMPUTER SIMULATION

This section mainly verifies the performance and authenticity of the algorithm proposed in this paper through several sets of simulation experiments. For the convenience of description, the algorithm proposed in this paper is referred

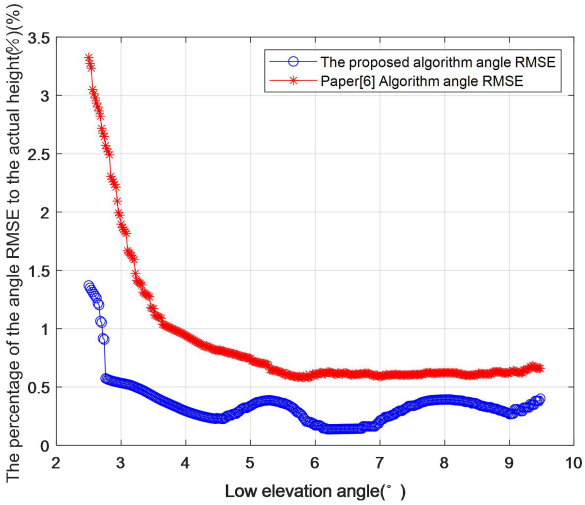

(a) Angle percentage chart

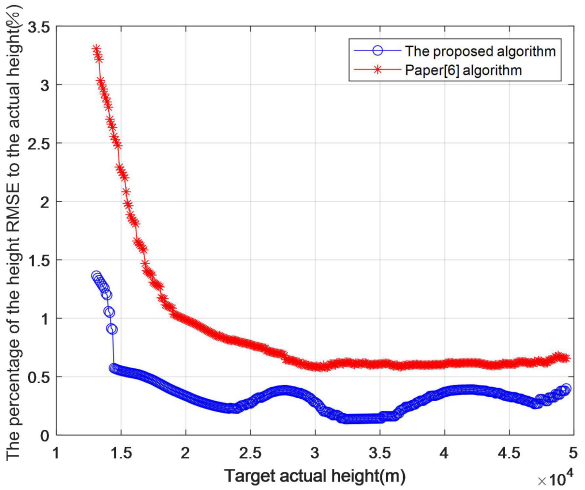

(b) Height percentage chart

FIGURE 10. RMSE percentage diagram.

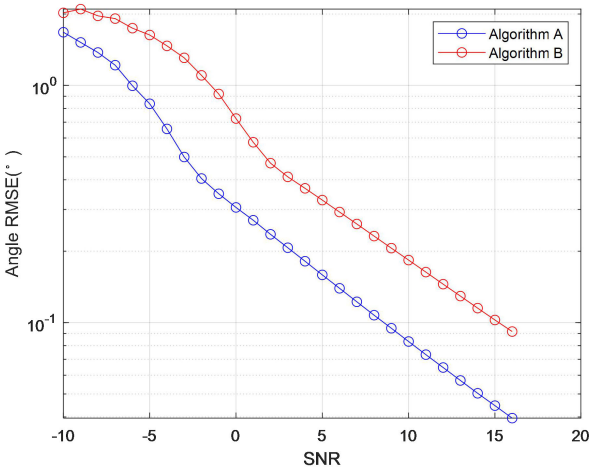

(a) The angle RMSE changes with the SNR

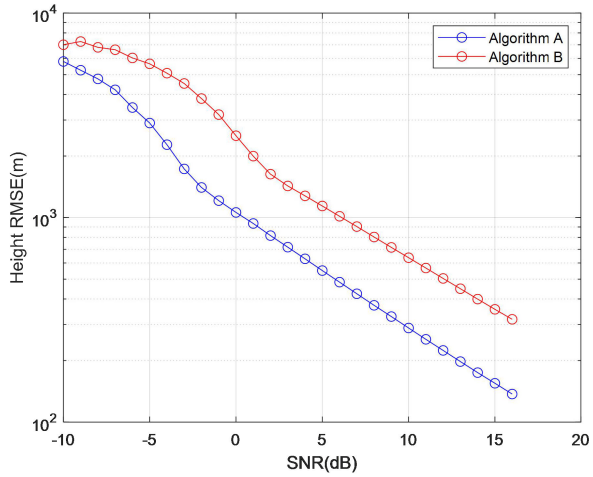

(b) The height RMSE changes with the SNR

FIGURE 11. RMSE changes with SNR.

to as algorithm A, and the algorithm proposed in paper [6] is referred to as algorithm B. In this section, the Monte Carlo number K = 1000, and the target slope distance R = 200 km.

Consider a MIMO radar system with a co-located transceiver. The operating frequency is 180MHz, the number of transceiver elements is $M = N = 3$, and the element height is $H_1 = 4m$, $H_2 = 6m$, $H_3 = 9m$. The target wave elevation range is $2.5° \sim 9.5°$, and the interval is $0.02°$.

Fig. 8 is a comparison diagram of the arrival angle estimation result of the algorithm A proposed in this paper and the actual elevation angle value, and the SNR is 10dB. It can be seen from Fig. 8 that the algorithm proposed in this paper can accurately measure the target low elevation angle, and then obtain an accurate target height.

Fig. 9 is the RMSE graph of algorithm A and algorithm B, the SNR is 10dB. Fig. 9 (a) is the RMSE graph of the angle. From Fig. 9 (a), it can be found that the RMSE of algorithm A is smaller than that of algorithm B, which proves the superiority of the algorithm in this paper. In addition, from the Fig. 9 (b), it can be found that a smaller angle error will also lead to a larger height error. Therefore, compared with algorithm B, algorithm A has better measurement accuracy in the area of low elevation angle.

Fig. 10 is a percentage diagram of Algorithm A and Algorithm B. Its value is the ratio of the RMSE value the algorithm to the actual value, and the SNR is 0dB. It can also be found from Fig. 6 that the accuracy of algorithm A is higher than algorithm B. In addition, it can be found that only algorithm A has a RMSE of less than 1% when the SNR is 0dB, which is within 2% of the actual measurement accuracy requirements.

Fig. 11 is the RMSE graph of algorithm A and algorithm B, which changes with the change of SNR. It is not difficult to find that the RMSE of the two algorithms decreases with the increase of the SNR, but the RMSE of algorithm A is lower than that of algorithm B. In addition, when the SNR is low, compared with algorithm B, algorithm A has higher angle measurement and higher accuracy, so it can be proved that algorithm A has better robustness under low SNR.

VI. SUMMARY

In this paper, a signal model suitable for the MIMO radar beam splitting algorithm is derived, and the beam splitting phenomenon of the MIMO radar is analyzed. According to the expansion characteristics of the MIMO radar virtual array element, a virtual sub-array-level beam splitting algorithm based on the MIMO radar is proposed. The proposed algorithm improves the feasibility of MIMO radar low elevation angle height measurement. In addition, this paper simply derives the error value calculation formula and signal model of the proposed algorithm under complex terrain. The algorithm in this paper firstly establishes an error graph according to the radar frequency, antenna height and the reflection coefficient of the surrounding site of the radar; then combines the nine virtual channels into three channels, and uses the phase difference of the adjacent channels to perform low-elevation encoding confirm the target elevation angle range; then calculate the amplitude error value of the actual signal and compare the error curve chart established in advance to obtain the target low elevation angle; finally obtain the target height data according to the geometric relationship.The simulation results show that, compared with the algorithm proposed in [6], the algorithm proposed in this paper has better robustness and angle measurement accuracy under low SNR and strong interference conditions. When the SNR reaches 0dB, the measurement accuracy of the algorithm in this paper can still reach one percent of the target height. In summary, the algorithm in this paper has a very small amount of calculation and is easy to implement. In the next step, we will focus on the low-elevation height measurement algorithm under complex terrain.

REFERENCES

[1] H. Kuschel, "VHF/UHF radar. Part 1: Characteristics," *Electron. Commun. Eng. J.*, vol. 14, no. 2, pp. 61–72, Apr. 2002.

[2] H. Kuschel, "VHF/UHF radar. Part 2: Operational aspects and applications," *Electron. Commun. Eng. J.*, vol. 14, no. 3, pp. 101–111, Jun. 2002.

[3] H. Darvishi and M. A. Sebt, "Adaptive hybrid method for low-angle target tracking in multipath," *IET Radar, Sonar Navigat.*, vol. 12, no. 9, pp. 931–937, Sep. 2018.

[4] Z.-H. Xu, Z. Xiong, J.-N. Wu, and S.-P. Xiao, "Low-angle tracking algorithm using polarisation sensitive array for very-high frequency radar," *IET Radar, Sonar Navigat.*, vol. 8, no. 9, pp. 1035–1041, Dec. 2014.

[5] J. Tan, Z. Nie, and S. He, "A novel precise angle measurement for meter-wave radar based on multipath cancellation," in *Proc. CIE Int. Conf. Radar (RADAR)*, Guangzhou, China, Oct. 2016, pp. 1–4.

[6] B.-X. Chen, T.-J. Hu, Z.-L. Zheng, F. Wang, and S.-H. Zhang, "Method of altitude measurement based on beam split in VHF radar and its application," *Dianzi Xuebao*, vol. 35, no. 6, pp. 1021–1025, Jun. 2007.

[7] Y. Liu, H. Liu, X.-G. Xia, L. Zhang, and B. Jiu, "Projection techniques for altitude estimation over complex multipath condition-based VHF radar," *IEEE J. Sel. Topics Appl. Earth Observ. Remote Sens.*, vol. 11, no. 7, pp. 2362–2375, Jul. 2018.

[8] H. Xiang, B. Chen, M. Yang, and C. Li, "Altitude measurement based on characteristics reversal by deep neural network for VHF radar," *IET Radar, Sonar Navigat.*, vol. 13, no. 1, pp. 98–103, Jan. 2019.

[9] S. Huan, M. Zhang, G. Dai, and H. Gan, "Low elevation angle estimation with range super-resolution in wideband radar," *Sensors*, vol. 20, no. 11, p. 3104, May 2020.

[10] J. Li, D. Jiang, and X. Zhang, "DOA estimation based on combined unitary ESPRIT for coprime MIMO radar," *IEEE Commun. Lett.*, vol. 21, no. 1, pp. 96–99, Jan. 2017.

[11] J. Li and D. Jiang, "Low-complexity propagator based two dimensional angle estimation for coprime MIMO radar," *IEEE Access*, vol. 6, pp. 13931–13938, 2018.

[12] S. Qin, Y. D. Zhang, and M. G. Amin, "DOA estimation of mixed coherent and uncorrelated targets exploiting coprime MIMO radar," *Digit. Signal Process.*, vol. 61, pp. 26–34, Feb. 2017.

[13] J. Xu, W.-Q. Wang, and R. Gui, "Computational efficient DOA, DOD, and Doppler estimation algorithm for MIMO radar," *IEEE Signal Process. Lett.*, vol. 26, no. 1, pp. 44–48, Jan. 2019.

[14] J. Shi, G. Hu, B. Zong, and M. Chen, "DOA estimation using multipath echo power for MIMO radar in low-grazing angle," *IEEE Sensors J.*, vol. 16, no. 15, pp. 6087–6094, Aug. 2016.

[15] Y. Liu, B. Jiu, X.-G. Xia, H. Liu, and L. Zhang, "Height measurement of low-angle target using MIMO radar under multipath interference," *IEEE Trans. Aerosp. Electron. Syst.*, vol. 54, no. 2, pp. 808–818, Apr. 2018.

[16] L. Mao, H. Li, and Q. Zhang, "Transmit design and DOA estimation for wideband MIMO system with colocated nested arrays," *Signal Process.*, vol. 152, pp. 63–68, Nov. 2018.

[17] P. Lu and J. Wu, "Some issues on VHF MIMO radar system design," *Radar Sci. Technol.*, vol. 15, no. 3, pp. 236–240,246, Jun. 2017.

[18] S. Hong, Z. Zhao, M. Yan, Y. Wang, J. Zeng, and C. Zhang, "Low angle estimation with colored noise in bi-static MIMO radar," in *Proc. 11th Int. Symp. Antennas, Propag. EM Theory (ISAPE)*, Guilin, China, Oct. 2016, pp. 866–868.

[19] J. Liu, Z. Liu, and R. Xie, "Low angle estimation in MIMO radar," *Electron. Lett.*, vol. 46, no. 23, pp. 1565–1566, Nov. 2010.

[20] R. Schmidt, "Multiple emitter location and signal parameter estimation," *IEEE Trans. Antennas Propag.*, vol. AP-34, no. 3, pp. 276–280, Mar. 1986.

[21] J. Li, "Improved angular resolution for spatial smoothing techniques," *IEEE Trans. Signal Process.*, vol. 40, no. 12, pp. 3078–3081, Dec. 1992.

[22] W.-J. Zhang, Y.-B. Zhao, and S.-H. Zhang, "Altitude measurement of meter-wave radar using the general MUSIC algorithm and its improvement," *J. Electron. Inf. Technol.*, vol. 29, no. 2, pp. 387–390, Feb. 2007.

[23] J. Tan and Z. Nie, "Polarisation smoothing generalised MUSIC algorithm with PSA monostatic MIMO radar for low angle estimation," *Electron. Lett.*, vol. 54, no. 8, pp. 527–529, Apr. 2018.

[24] M. Djeddou, A. Belouchrani, and S. Aouada, "Maximum likelihood angle-frequency estimation in partially known correlated noise for low-elevation targets," *IEEE Trans. Signal Process.*, vol. 53, no. 8, pp. 3057–3064, Aug. 2005.

[25] S. Haykin, J. Reilly, and D. Taylor, "New realisation of maximum likelihood receiver for low-angle tracking radar," *Electron. Lett.*, vol. 16, no. 8, pp. 288–289, Apr. 1980.

[26] Y.-H. Choi, "Alternating projection for maximum-likelihood source localization using eigendecomposition," *IEEE Signal Process. Lett.*, vol. 6, no. 4, pp. 73–75, Apr. 1999.

[27] T. Lo and J. Litva, "Use of a highly deterministic multipath signal model in low-angle tracking," *IEE Proc. F, Radar Signal Process.*, vol. 138, no. 2, pp. 163–171, Apr. 1991.

[28] E. Bosse and R. M. Turner, "Height ambiguities in maximum likelihood estimation with a multipath propagation model," in *Proc. 22nd Asilomar Conf. Signals, Syst. Comput.*, Pacific Grove, CA, USA, 1988, pp. 690–695.

[29] S. Wang, Y. Cao, H. Su, and Y. Wang, "Low angle estimation for MIMO radar with arbitrary array structures," *Int. J. Electron. Lett.*, vol. 7, no. 4, pp. 422–433, Oct. 2019.

[30] J. Shi, G. Hu, and T. Lei, "DOA estimation algorithms for low-angle targets with MIMO radar," *Electron. Lett.*, vol. 52, no. 8, pp. 652–654, Apr. 2016.

[31] J. Tan, Z. Nie, and S. Peng, "Adaptive time reversal MUSIC algorithm with monostatic MIMO radar for low angle estimation," in *Proc. IEEE Radar Conf. (RadarConf)*, Boston, MA, USA, Apr. 2019, pp. 1–6.

[32] B.-X. Chen, G.-D. Liu, and S.-H. Zhang, "Method of altitude measurement based on beam split in multi-antenna VHF radar," in *Proc. Int. Conf. Radar Syst. (RADAR)*, Toulouse, France, 2004, pp. 1–5.

[33] M. L. Meeks, *Radar Propagation at Low Altitudes*. Dedham, MA, USA: Artech House, 1982, p. 24897.

[34] P. Beckmann and A. Spizzichino, *The Scattering of Electromagnetic Waves From Rough Surfaces*. Norwood, MA, USA: Artech House, 1987.

[35] G. Uyar, "Low elevation target detection and direction finding," M.S. thesis, Middle East Tech. Univ., Ankara, Turkey, 2012.

[36] E. Daeipour, W. D. Blair, and Y. Bar-Shalom, "Bias compensation and tracking with monopulse radars in the presence of multi path," *IEEE Trans. Aerosp. Electron. Syst.*, vol. 33, no. 3, pp. 863–882, Jul. 1997.

CHEN CHEN was born in Xi'an, Shaanxi, China, in 1997. He received the bachelor's degree from Xidian University, in 2019. He is currently pursuing the master's degree with Air Force Engineering University. Since 2019, he has been a Research Assistant with the Tracking Guidance Teaching and Research Section.

JIANFENG TAO was born in Xi'an, Shaanxi, China, in 1963. He is currently a Professor and a Postgraduate Tutor with Air Force Engineering University. His main research interests include radar system analysis and simulation.

GUIMEI ZHENG was born in Fuzhou, Fujian, China, in 1987. He is currently an Associate Professor with Air Force Engineering University. His research interest includes array space spectrum estimation algorithms.

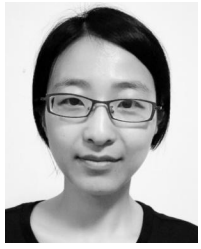

YUWEI SONG was born in Dalian, Liaoning, China, in 1986. She is currently pursuing the Ph.D. degree. Her research interest includes MIMO radar spectrum estimation.